Crowding Effects on the Segregation of Cylindrically Confined Ring Polymers

By

Deanna Rita-Mae Kerry

University of Prince Edward Island

Charlottetown, PE, Canada

A thesis submitted in partial fulfillment of

the requirements for the Honours Programme

in the Department of Physics

This Thesis is Approved

Signature (Supervisor)	Date
Signature (Second Reader)	Date

This Thesis is Accepted

Signature (Dean of Science)	Date

Abstract

In the cell cycle, chromosome segregation occurs during anaphase, the process where original and replicated chromosomes move towards opposite sides of the cell to await cell division. This process is well-described and understood in eukaryotic cells, but this is not true for bacteria. Bacteria do not have the structures to facilitate chromosome segregation that are present in eukaryotes. Some researchers have suggested that instead of being facilitated by specific structures, bacterial chromosome segregation is driven largely by entropy.

We modeled bacterial chromosomes as hard-sphere ring polymers and studied systems of two polymers in cylindrical confinement of both finite and infinite length. The polymers have lower entropy when they overlap along the cylinder than when they are completely segregated, which means that they segregate spontaneously from one another in order to achieve equilibrium (where in this type of system, entropy is maximized).

Because up to 30% of the volume of certain bacterial cells can be occupied by macromolecular crowders, it was important to consider the effects of crowding agents on our system. A previous study observed that the free energy barrier of segregating polymers decreases with increasing crowding agent density, and we were able to reproduce this trend for polymers of different size, cylinder diameter, and crowding agent density. We also studied the effects of crowding on polymers confined to a cylinder of finite length and observed that the free energy barrier increases with increasing crowding agent density, a trend that was opposite to observations from the infinitely long cylinder.

Acknowledgments

I would like to thank Dr. Polson for his guidance and advice during the past two years, and especially during this Honours project. His swift and constructive feedback was extremely helpful while writing this thesis, and I could always count on him to provide clear and helpful answers whenever I needed them. I would also like to thank the UPEI Physics Society for being such a supportive group of friends during these last few busy years. Through late nights working in the lounge, endless presentation rehearsals, and constant AUPAC meetings, we still managed to get along perfectly and get things done on time. Joining the society was one of the best decisions I made when I started this degree, and I look forward to seeing what brilliant things these people go on to do. So thank you to Patrick Strongman, Phoenix McCloud, Aidan Tremblett, Andrew Cameron, Patrick Connolly, Dayna Brown, Willow M'Cloud, Zak McLure, David Heckbert, Eduardo Egger, Jonathan Horrocks, Kyle Bryenton, and Keegan Marr for their friendships and support.

Finally, a special shout-out to Nancy Ramsay for believing in me since Day 1 of this degree. You'll always be my best friend.

Contents

List of Figures

Chapter 1

Introduction

1.1 Relevant Work

The replication of DNA allows organisms to pass their genetic information on to their next generation of cells. The process of DNA replication and separation during cell division happens in both eukaryotic and prokaryotic cells[1]. Prokaryotic cells are small, simple cells that include archaea and bacteria. These types of cells do not contain membrane-bound organelles or nuclei. Eukaryotic cells are cells with much more complex internal structure that, in constrast, contain membrane-bound organelles and nuclei. Animals and plants are made up of eukaryotic cells[2]. Figure 1.1 compares the general structure of prokaryotic and eukaryotic cells. In eukaryotes, the separation of chromosomes (structures made up of chromatin, which are complexes of DNA and protein) occurs with aid from spindles originating from structures called centrioles, along with various proteins such as kinetochores [4]. While the mechanisms behind eukaryotic chromosome segregation during mitosis has been considerably well-

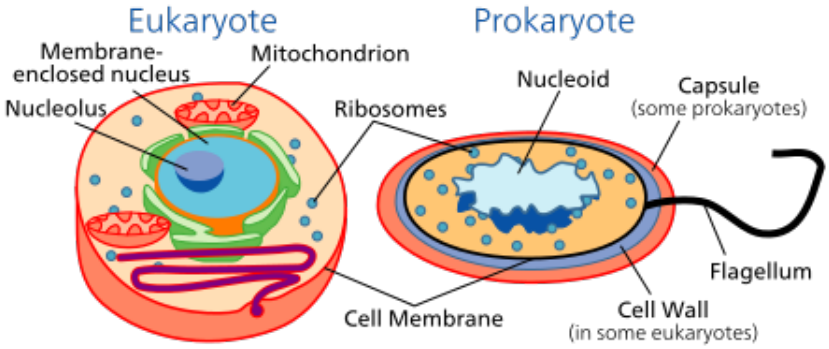

Figure 1.1: Illustration of prokaryotic and eukaryotic cells[3]. The eukaryotic cell is much more complex and includes membrane-bound organelles and a nucleus. The prokaryotic nucleoid is the general region where the chromosomes are located.

understood for a number of years[5], the same cannot be said for bacterial chromosome segregation. Chromosome segregation in bacteria does not have a comprehensive explanation[4,5,7-10]. To better understand bacterial chromosome segregation, we look to the field of polymer physics to provide us with concepts and models that may be very important in understanding the relevant mechanisms involved.

At the most basic level, polymers are molecules of repeating chemical units called monomers. These units are clusters of covalently bonded atoms. There are a number of different polymer topologies, such as linear polymers (ends not connecting), ring polymers (monomers connected together in a ring), and branched polymers. Many different compounds can be considered polymers, including chromosomes (see Figure 1.2, an electron micrograph of a bacterial chromosome.) Chromosomes are particularly good examples of polymeric systems to study for a number of reasons: each strand after replication is exactly the same length as before, bacterial chromosomes are naturally-occuring examples of ring polymers that are difficult to create artificially,

and DNA can be stained and thus examined at the molecular level very easily[13]. Combine these factors with the gaps in our knowledge of chromosome behavior and it is clear why polymer physics is deeply relevant to the study of chromosomes.

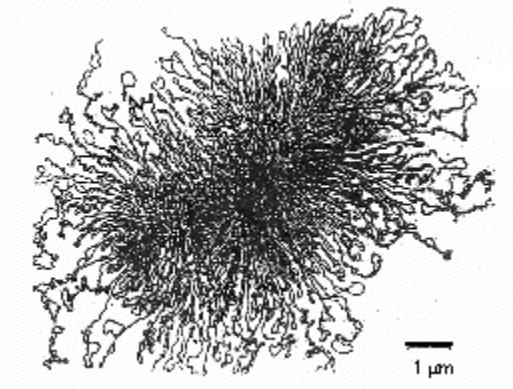

Figure 1.2: Electron micrograph of a bacterial chromosome[11]. Bacterial chromosomes are very long strands of ring-shaped DNA.

Paul Flory is considered to be a pioneer in the field of polymer physics, and he introduced a number of key polymeric concepts during his career. The concept of excluded volume is particularly important in this thesis, and it was Flory who connected the idea to polymers in the early 1950s[14, 15]. The concept is simply that a molecule (for example, a polymer) occupies a certain volume in space and thus prevents any portion of other molecules from occupying that particular volume. If more molecules are added to the system, there is greater excluded volume. This idea forms the basis for more complex ideas in polymer physics– in particular, the nature of segregating polymers in confinement.

The explicit connection between polymers and chromosomes did not come until over half a century after Flory's initial work. However, a paper published by Daoud

and De Gennes in 1977 considers the scenario of polymers confined to slits and tubes, and even considers many polymers confined to a capillary [16], not unlike the scenario of two polymers confined to cylinders as considered in this study. Computational modeling was of course extremely limited in 1977, so although multiple polymers trapped in long confinements was treated theoretically many decades ago, there would not be computer simulations of this problem until many years later.

Confined polymers have been studied both computationally and experimentally. This is useful not only in the study of bacterial chromosomes, but in other areas of microbiology, such as DNA translocation[17, 18, 19], that may have applications in DNA sequencing. Confined polymers have less available space and therefore can sample fewer possible configurations. This means that the entropy of a confined polymer will be much lower than the entropy of a free polymer. Experiments allow theoretical models to be tested, and both experiment and theory show that linear polymers and ring polymers behave in distinct ways inside narrow confinements[20]. This topic will be explored in this and other chapters.

A computational study by Jun and Mulder in 2006 made the connection between confined polymer behavior and chromosomes in bacteria[6]. The authors argued that conformational entropy was a major factor in what caused bacterial chromosomes to segregate. They carried out a simulation where two polymers were confined to a infinitely long narrow tube that drastically changed the conformational behaviour relative to the case of no confinement. When the polymers are close to one another, they crowd each other and the conformational entropy is reduced. Conformational entropy provides a measure of the number of molecular configurations available to the system (this will be explained further in the next chapter). The reduction in

conformational entropy drives the polymers to segregate from one another. They performed additional simulations with polymers confined in a tube of finite length to more realistically model the shape of rod-shaped bacteria, with some of the simulations using ring-shaped polymers to model the ring topology of actual bacterial chromosomes. Both the linear and ring polymers were found to segregate in the tube of finite length, with the ring polymers separating more strongly from one another. The authors argued that these results show that entropy must be considered when studying the bacterial chromosome. More studies were required, however, because computational resources were not quite at the level they needed to be to gather extensive quantitative data when this paper was published[6].

In 2010, Jun and Wright examined once again the role of conformational entropy in segregating chromosomes [7]. Here, the role of bacterial proteins was considered and their role in segregation, and how it relates to entropic forces was discussed. The authors argued that the proteins present do not actively participate in the segregation themselves, as the chromosomes are so large compared to the proteins that it likely is not possible for them to directly cause such large conformational changes in the chromosomes. They suggested instead that the proteins merely create the conditions (e.g. chromosome alignment) under which the chromosomes can segregate by the previously established entropic method, and in some cases provide active transport at the very end of segregation[7]. The role of proteins more generally on polymer segregation is a theme that appears again both in this thesis and other literature [21][22].

Subsequent research connecting molecular biology with polymer physics often addressed the connection between chromosome segregation and entropy. Studying the

organizational structure of the *E. coli* chromosomes showed that these chromosomes are linearly ordered[23], which is the regime of monomer organization that most easily allows confined polymers to segregate. Linear ordering is the linear relation between a monomer's average position along the long axis of the confining space and its location along the length of the contour of the polymer. In addition to linear polymers, this organization exists in ring polymers, which can be visualized as two linear polymers in parallel with one another. However, it must be noted that segregation still occurs to some extent in the absence of linear ordering[8]. Nevertheless, it is promising that chromosomes exist within the region most suited to polymer confinement.

There have also been studies on the confinement of ring polymers[10][24]. Under cylindrical confinement, replacing a linear polymer with a ring polymer effectively reduces the diameter of confinement the polymer experiences (The ring polymer must have at least two monomers next to each other in the x–y plane inside of a confinement along the z axis, as opposed to just one with a linear polymer). This is a particularly relevant result because more confined polymers have a higher tendency to segregate[8][12].

We return to the concept of crowding agents and what effects they might have on bacterial chromosomes. Some evidence suggests that crowding agents that exist in bacterial cells such as ribosomes or other proteins compact the chromosomes into a occupying a smaller volume, a relevant effect due to the enormous size of chromosomes compared to the cell that contains them[25]. This effect does not cause a decrease in the total entropy, however, because while it reduces the polymer's conformational entropy, its translational entropy is greatly increased because the centre of mass of a condensed chromosome can now occupy many more locations [26]. Furthermore,

since there are a very large number of proteins in bacterial cells such as *E. coli*, it inevitably means that proteins and chromosomes come into contact with one another very frequently. It therefore suggests that the role of proteins within the cell is not only to perform complex biological reactions, but simply to occupy more volume and cause the chromosomes to condense [27, 28, 29, 30]. Attractive interactions between crowding agents and polymers have also been shown to aid polymer segregation[30].

Jun argues that molecular crowding should not affect the segregation of bacterial chromosomes[31]. The crowding agents have two opposing effects on the two confined chromosomes. First, the two polymers will be condensed by the crowding agents, and such a crowded configuration will have a high free energy. Thus, the chromosomes will want to segregate to reduce their free energy and gain conformational entropy. However, the crowding agents exert a force on the polymers that will cause them to mix. These effects effectively "cancel out" and thus molecular crowding should not have any effect on segregation [31].

There are simulation results that contradict this prediction, however. Shin *et al.* examined the effects of molecular crowding on polymer segregation in their 2014 work and found that rather than having a neutral effect, as Jun et al. claim, the crowding agents actually help facilitate ring polymer segregation in a confining cylinder[21]. That this work is at odds with the previous prediction[31] warrants further investigation into how crowding agents affect polymer segregation. It must be noted, however, that Jun's calculations are only approximate, and consider only polymers in free space rather than confined polymers. We will examine such effects in this thesis, and the specifics are outlined at the end of the introduction.

One of the explanations in the latter work is also problematic[21]. The authors

measured the effect of crowding agent concentration on the segregation free energy function, and observed that the overlap free energy barrier decreases as crowding agent concentration increases. That is, the difference in free energy between overlapping and nonoverlapping configurations was reduced. The proposed reason for this is that at higher agent concentration, the "presence of crowding agents slows down the dynamics of the polymer-crowder system"[21]. However, this explanation suggests that their result is specific to the dynamics of the system. In equilibrium systems, however, the probability distributions should be independent of the dynamics. The explanation therefore does not make sense. We repeated this simulation using a different technique and discuss another possible explanation in chapter 4.

The simulations and discussion in this thesis follow directly from work completed by Polson and Montgomery[10]. In this recent study, the free energy of two polymers confined to an infinitely long cylinder was examined. Monte Carlo simulations were used to calculate the free energy as a function of polymer overlap along the cylinder. This was one of the first studies that examined the free energy functions of two overlapping polymers with regards to the size of the confining cylinder, the number of monomers in each polymer, the volume the polymers occupied, and the rigidity of the polymer[10]. Using the Self-Consistent Histogram Method[32] the free energy functions were calculated from the probability distributions related to the polymer behaviour[10]. This method was used in Polson's previous work on polymer translocation [33][34][35] and is the first time it was used to calculate free energy functions for the process of polymer segregation. The Self-Consistent Histogram Method is necessary in these calculations in order to avoid poor statistics due to high free energy barriers. The methods used to calculate free energy functions in these papers will

also be used in this thesis, and they will be described in detail in a later chapter.

The simulations of the linear polymers in cylindrical confinement showed that free energy was maximized when the polymers' centres of mass were completely overlapping, and minimized when they were far apart. When the two polymers are confined to an infinitely long cylinder, the free energy remains low as the centres of mass move away. In cylinders of finite length, however, the free energy increases again as the polymers reach the ends of the confinement[10].

1.2 My Contribution

This thesis focuses on determining the free energy changes in a system of two polymers confined to a cylinder. Because we are motivated by the segregation of two chromosomes within a bacterial cell (particularly *E. coli*), we will focus on ring polymers. We will incorporate crowding agents to represent molecular objects, such as proteins, that are thought to aid in chromosome segregation.

Our system of two ring polymers confined with crowding agents will be considered in both an infinitely long cylinder and a cylinder of finite length. The former is useful in focusing specifically on the physics surrounding segregation in lateral confinement; however, the latter will be examined afterwards as it is more physically relevant to the problem of bacteria.

Finally, we will discuss the effects of crowding agents on polymer segregation and discuss changes in the free energy function with increased crowding agent concentration, as mentioned previously in this chapter.

1.3 Thesis Outline

The next chapter focuses on the theoretical background relevant to the project. It will discuss the entropy and free energy, the basics of polymer physics, and the effects of polymers under confinement. Chapter 3 will outline the model and simulation methodology, including the simulation structure and calculation methods. Chapter 4 will present the results and discuss their meaning. We conclude the thesis in Chapter 5 and summarize the findings of the project. We also suggest future work that follows from the results.

Chapter 2

Theory

2.1 Polymers

Polymers are molecules made up of repeating chemical sub-units called monomers. The sub-units may be the same, in which case the polymer is called a homopolymer, or they may be different, in which case it is a heteropolymer. The number of monomers within a polymer can influence its behaviour: for example, hydrocarbons can have different numbers of monomers (carbon and hydrogen molecules). Short hydrocarbons that are less than 15 monomers exist at room temperature as a gas or low viscosity liquid, whereas very long hydrocarbons that are over 1000 monomers exist as solid plastic[36]. Polymers are also found in biology, a notable and relevant example being DNA found in all living organisms, such as the ring polymer DNA of the *E. coli* cell mentioned in the previous chapter.

We will begin by considering the ideal chain model of a linear polymer, which describes the monomers as non-interacting particles. We can calculate the end-to-

end vector, $\vec{R}_{\mathrm{e}}$, of a linear polymer using

$$\vec{R}_{\mathrm{e}} = \vec{r}_N - \vec{r}_1 \tag{2.1}$$

where $\vec{r}_1$ is the coordinate of the first monomer and $\vec{r}_N$ is the coordinate of the last monomer in a polymer of N monomers. In this form, however, the equation is not particularly useful. These polymers are typically very flexible and can take on many different conformations. In order to account for these different conformations of a polymer, we must take into consideration the ensemble average, which is an average of all possible states. The average end-to-end distance is the root-mean-square of equation (2.1):

$$\bar{R}_{\mathrm{e}} = \sqrt{\langle |\vec{R}_{\mathrm{e}}|^2 \rangle} = \sqrt{\langle |\vec{r}_N - \vec{r}_1|^2 \rangle}. \tag{2.2}$$

We can also calculate the radius of gyration, which is the root-mean-square distance between the centre of mass of the polymer and its monomers. This is an especially useful quantity for polymers such as ring polymers that do not have a well-defined end-to-end distance. The radius of gyration is defined as

$$\bar{R}_{\mathrm{g}} = \sqrt{\left\langle \frac{1}{N} \sum_{i=1}^{N} |\vec{r}_i - \vec{r}_{\mathrm{cm}}|^2 \right\rangle}, \tag{2.3}$$

where $\vec{r}_{\mathrm{cm}}$ is the coordinate of the centre of mass of the polymer,

$$\vec{r}_{\mathrm{cm}} = \frac{1}{N} \sum_{i=1}^{N} \vec{r}_{\mathrm{i}},$$

assuming the monomers have equal mass. The end-to-end distance and the radius of gyration both measure the average size of the polymer. The smaller these values are, the more tightly compacted the polymer is.

These values change with the number of monomers in the polymer. In any polymer model, more monomers result in a larger end-to-end distance and radius of gyration. We can express very generally the relationship as[36]

$$\bar{R}_{\mathrm{e}} \sim N^{\nu} \tag{2.4}$$

$$\bar{R}_{\mathrm{g}} \sim N^{\nu}, \tag{2.5}$$

where N is the number of monomers in a polymer and ν is a scaling exponent. This equation means that these measures of polymer size are proportional to some value N^{ν}. Both the end-to-end distance and the radius of gyration have the same scaling exponent ν.

The ideal chain model has a scaling exponent of $\nu = \frac{1}{2}$[36]. However, the ideal chain model does not closely approximate a real polymer. Real polymers have solid monomers that cannot overlap with one another, which the ideal chain model does not account for. This leads to the concept of a self-avoiding polymer that more accurately reflects reality. Self-avoiding chains have a larger end-to-end distance and radius of gyration than the ideal chain, because the monomers occupy space and their centres of mass cannot get as close to one another.

This model assumes 'good solvent' conditions, which means that interactions between the monomers and solvent are favourable and the polymer tends to spread out to increase contact with the solvent. This is in contrast to 'poor solvent' conditions, in which monomer-monomer interactions are favourable, meaning there is an effective attraction between monomers that can cause the polymer to form compact shapes. In good solvent, polymers have a scaling exponent of $\nu \approx 0.588$, which is often approximated as $\nu = \frac{3}{5}$[38]. There are additional possible interactions between

monomers, including attractive and repulsive forces. For example, one could consider hydrogen bonding, electrostatic attraction/repulsion, etc. This is especially useful when considering molecules that have very strong attractive or repulsive properties. However, we choose not to consider such interactions in this study. The excluded volume interactions are sufficient to capture the physics thought to be relevant in many experimental systems.

2.2 Thermodynamics

There are a number of thermodynamic quantities important in statistical physics. One of the most important is entropy (S), which can be written

$$S = k_B \ln\Omega. \tag{2.6}$$

Entropy can be described as being proportional to "the logarithm of the number of ways of arranging things in a system"[37]. The number of ways of "arranging things" in the case of a polymer is the multiplicity (Ω), or number of possible states of the polymer. This could include the possible conformational states of the polymer (that is, the number of shapes) or the possible translational states of the polymer (where the polymer exists in space). However, only the former is relevant to this study, so we choose Ω to only include the number of possible conformational states of the polymer.

The Helmholtz free energy is another important thermodynamic quantity in polymer physics. It is the amount of energy available to do work when the temperature (T) and volume (V) are fixed. The Helmholtz free energy (F) of a system can be written

$$F = U - TS, \tag{2.7}$$

where U is the average total energy.

Consider a quantity λ that depends on the configuration of a system of N particles, i.e. $\lambda = \lambda(\vec{r}^N)$. This leads to a parameterization of the entropy:

$$S(\lambda) = k_B \ln\Omega(\lambda), \tag{2.8}$$

and this, in turn, leads to a parameterization of free energy,

$$F(\lambda) = U(\lambda) - TS(\lambda), \tag{2.9}$$

where T is constant (see Chapter 3). The total average energy $U(\lambda)$ is the sum of the kinetic and potential energy. According to the equipartition theorem, the average kinetic energy of a system of N molecules, with $3N$ degrees of freedom, at equilibrium is $\frac{3}{2}Nk_{\mathrm{B}}T$, but in our system the temperature is constant. The kinetic energy is therefore invariant to changes in λ and can be ignored, resulting in U simply becoming the potential energy. However, for a polymer described by an athermal model such as a hard-sphere chain, the potential becomes

$$U = \begin{cases} \infty, & \text{if any polymers overlap} \\ 0, & \text{otherwise} \end{cases} \tag{2.10}$$

The monomers will never overlap, so $U = 0$. Equation (2.9) then becomes

$$F(\lambda) = -TS(\lambda), \tag{2.11}$$

where we can see the relationship between free energy and energy in an athermal, hard-sphere polymer model: as entropy decreases, free energy increases linearly. This concept is very relevant to the work that follows, and will be used many times when interpreting the results in Chapter 4.

For a system in state s, the probability that it can be found in this state is given by:

$$P_s = \frac{\exp\left[-E_s/k_BT\right]}{Z}, \tag{2.12}$$

where Z is the partition function:

$$Z = \sum_s \exp\left[-E_s/k_BT\right], \tag{2.13}$$

In this study, a sum over microstates becomes an integration over coordinates. If we want the probability distribution for the *energy* of a system, we must multiply equation (2.12) by the multiplicities of states with energy E, yielding

$$P(E) = \Omega(E)\frac{\exp\left[-E/k_BT\right]}{Z}, \tag{2.14}$$

where Z can be written

$$Z = \int dE\Omega(E)\exp\left[-E/k_BT\right]$$

This means that $P(E)dE$ is the probability that the energy is within the range $[E, E+dE]$.

From equation (2.6), we can rewrite $\Omega(E)$ in terms of the entropy:

$$\Omega(E) = \exp\left(S(E)/k_B\right),$$

where

$$S(E) \equiv k_B \ln\Omega(E)$$

so that equation (2.14) becomes

$$P(E) = \frac{1}{Z}\exp\left[\frac{-(E - TS(E))}{k_BT}\right] \tag{2.15}$$

using the definition of F in equation (2.11), it follows that

$$P(E) = \frac{\exp\left[-F(E)/k_B T\right]}{Z} \tag{2.16}$$

where $F(E) = E - TS(E)$

Following a similar procedure, we can derive a more general relation as a function of some other quantity λ,

$$P(\lambda) \propto \exp\left(\frac{-F(\lambda)}{k_{\mathrm{B}} T}\right) \tag{2.17}$$

where $F(\lambda) \equiv E(\lambda) - TS(\lambda)$, where $E(\lambda)$ and $S(\lambda)$ are the energy and entropy calculated for states where λ is constrained to some value. This holds for a system at constant T and V. This can be rewritten as

$$F(\lambda) = -k_{\mathrm{B}} T \ln P(\lambda) + C \tag{2.18}$$

where C is a constant. The free energy is proportional to the probability that λ is a particular value. According to equation (2.18), if the probability that λ is a particular value is high, the free energy will be low (this is true for athermal models like the one used in this study). Recalling equation (2.11), this means the system is more probable to be in states that lead to high entropy.

2.3 Single Confined Polymer

Let us start by examining a polymer confined to an infinitely long tube. If the diameter (D) of the tube is sufficiently narrow ($\bar{R}_{\mathrm{g}} < D$), then the number of possible conformations (Ω) of the polymer will be reduced. This reduces the entropy, due to equation (2.8), and causes an increase in free energy, as we can see from equation (2.11).

It is possible to determine the relationship between the confinement diameter and the free energy[16]. This uses the blob model, a concept that models a confined polymer as a series of smaller, unconfined polymers, each consisting of an average of g monomers. Figure 2.1 illustrates this concept[39]. Each blob contains one of these smaller 'unconfined' polymers.

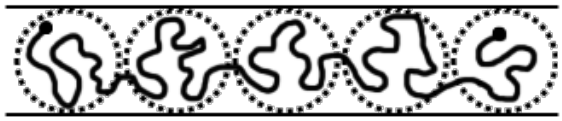

Figure 2.1: Blob model. Each circle is a blob.

The radius of gyration for each of these smaller polymers is roughly the radius of the confinement. This leads equation (2.5) to become

$$D/2 \sim g^{\nu}. \tag{2.19}$$

Since we are more interested in the scaling behaviour, we ignore the factor of $\frac{1}{2}$. Rearranging, we can write

$$g \sim D^{1/\nu}. \tag{2.20}$$

The number of monomers in each blob is determined by the diameter of the confinement. Noting that the total number of blobs is given by $n_{\text{blobs}} = N/g$, it follows that

$$n_{\text{blobs}} \sim ND^{-1/\nu}. \tag{2.21}$$

Each blob has free energy of the order of k_BT [36], so we can approximate the total free energy of the confined polymer:

$$F(N, D) \approx n_{\text{blobs}} k_{\text{B}} T \sim ND^{-1/\nu} k_{\text{B}} T \tag{2.22}$$

In 'good solvent' conditions, this leads to

$$F(N, D) \approx N D^{-5/3} k_{\mathrm{B}} T, \tag{2.23}$$

as $\nu \approx 3/5$. These approximations are valid when $g \gg 1$ and $n_{blobs} \gg 1$. This requires D to be large and N to be very large.

2.4 Two Confined Polymers

Consider now an infinitely long tube with two polymers inside. The distance between the polymers is measured along the cylinder by the location of the centres of masses, and is denoted by λ.

The centres of mass may be any distance from each other, including $\lambda = 0$. In this case the polymers are completely overlapping [1]. When they are not overlapping at all, as in Figure 2.2, they are unaffected by each other and behave like the confined single-polymer case described in the last section. This means that the total free

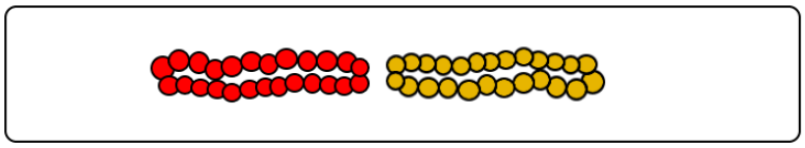

Figure 2.2: Polymers that are not overlapping at all. These polymers are unaffected by each other.

[1] Overlapping polymers in this case does not mean the same thing as overlapping monomers. The monomers still do not overlap.

energy of the system is the sum of two terms in the form of equation (2.23),

$$F(N, D) \approx 2ND^{-1/\nu}k_{\mathrm{B}}T = 2ND^{-5/3}k_{\mathrm{B}}T. \tag{2.24}$$

This is only the case when the polymers are "far away" from one another, so that they are not in contact.

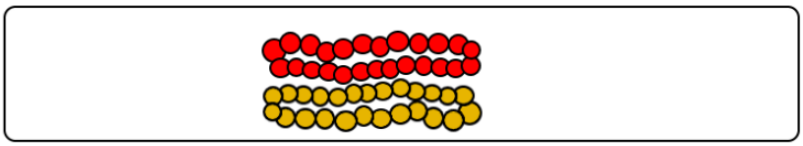

Figure 2.3: Polymers that are completely overlapping ($\lambda = 0$).

The free energy of a system of two confined, completely overlapping polymers, shown in Figure 2.3, ($\lambda = 0$) can be approximated as two polymers separately confined to a smaller diameter. In this model, each polymer is confined to a cylinder of half the cross-sectional area, which results in a new effective diameter of $D' = \frac{D}{\sqrt{2}}$[24]. The free energy of the system is then

$$F(\lambda = 0) = 2F(N, D/\sqrt{2}) \approx 2N(D/\sqrt{2})^{-1/\nu}k_{\mathrm{B}}T = 2^{11/6}ND^{-5/3}k_{\mathrm{B}}T, \tag{2.25}$$

where $\nu \approx \frac{3}{5}$ is used. The free energy is greater for overlapping polymers than for non-overlapping ones, as expected. We can estimate the scaling of the free energy barrier,

$$\Delta F = F(0) - F(\infty) \propto ND^{-5/3}. \tag{2.26}$$

Noting the relationship between free energy and entropy in equation(2.11), equations (2.24) and (2.25) tell us that the entropy is higher for non-overlapping polymers.

This in turn means that the system is more likely to be found in a state of non-overlap. Because systems at equilibrium have maximum entropy, if the polymers are overlapping they will segregate spontaneously to achieve this maximum entropy.

This concept also applies to ring polymers (which is the relevant polymer topology for this project). The free energy of a system of a single confined ring polymer with N monomers can be thought of as two overlapping linear polymers each of $\frac{N}{2}$ monomers. The free energy of a confined ring polymer is therefore

$$F_{ring} = 2F(N/2, D/\sqrt{2}) \approx 2\frac{N}{2}(D/\sqrt{2})^{-1/\nu}k_{\mathrm{B}}T = 2^{5/6}ND^{-5/3}k_{\mathrm{B}}T, \tag{2.27}$$

which we have determined from equation (2.25). The free energy of a system of two confined, completely non-interacting ring polymers is the sum of the free energy of each polymer:

$$F_{rings} \approx 2N(D/\sqrt{2})^{-1/\nu}k_{\mathrm{B}}T = 2^{11/6}ND^{-5/3}k_{\mathrm{B}}T, \tag{2.28}$$

which is the same result as the free energy for two overlapping linear polymers with N monomers each.

The free energy of a system of two confined, completely overlapping ring polymers ($\lambda = 0$) can then be approximated using the same logic as for linear polymers. This time it can be approximated as four polymers with $\frac{N}{2}$ monomers each separately confined to a smaller diameter. Each polymer is confined to a quarter of the cross-sectional area, which results in a new effective diameter of $D' = \frac{D}{2}$ for each 'linear polymer'. The free energy of the system of two confined ring polymers completely overlapping is then

$$F_{ring}(\lambda = 0) = 4F(N/2, D/2) \approx 2N(D/2)^{-1/\nu} k_{\mathrm{B}}T = 2^{8/3} N D^{-5/3} k_{\mathrm{B}}T \qquad (2.29)$$

The free energy for the system of two ring polymers is greater when the polymers are overlapping than when they are segregated, so the polymers will spontaneously segregate from one another. This is the proposed mechanism behind bacterial chromosome segregation discussed in Chapter 1.

2.5 Crowding Agents

This study examines systems with crowding agents, which are objects inside of the confinement that occupy space and crowd the polymers. We add crowding agents to the model to account for the high density of particles inside most bacterial cells (especially *E. coli*), where the volume is often between 20-30% occupied by macromolecular objects.

Whenever smaller particles are added to a system of larger particles, depletion forces must be accounted for. This is an entropic effect caused by the smaller particles that result in an effective attractive force between the larger particles, and it is always present regardless of any interactions between the crowding agents[40][41].

Consider a system of large spheres of diameter D in a solution of smaller spheres of diameter d. Both the large and small spheres are considered to be hard particles, so that the potential for interactions between like particles is

$$U(r) = \begin{cases} \infty, & r < \sigma \\ 0, & r \geq \sigma \end{cases} \tag{2.30}$$

where l is the distance between the centres of mass of two small particles or two large particles $\sigma = d$ for small particles and $\sigma = D$ for large particles.

Interactions between large and small particles are subject to the potential

$$U(r) = \begin{cases} \infty, & r < \frac{d+D}{2} \\ 0, & r \geq \frac{d+D}{2} \end{cases} \tag{2.31}$$

where r is the distance between the centres of mass of a large and small particle. None of the particles are therefore able to overlap with one another. The particles are illustrated in the Figure 2.4.

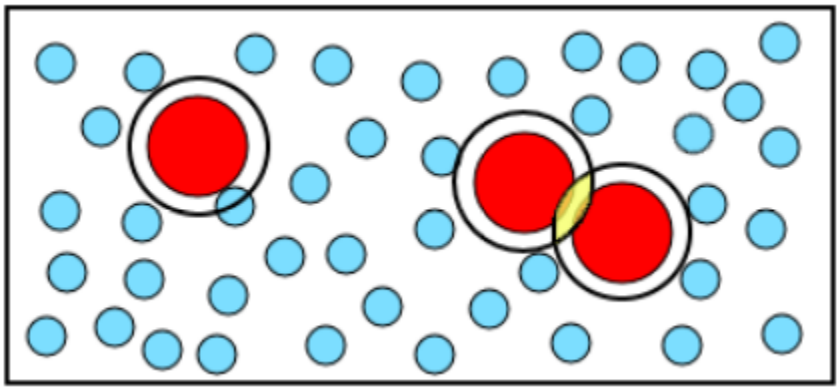

Figure 2.4: A mixture of large and small particles. The circular regions around the large red particles are excluded volume zones that are inaccessible to the smaller particles' centres of mass. The yellow area is a region of overlapping excluded volume zones.

The circles around the large particles are regions that the centres of mass of the small particles cannot occupy, due to the restrictions of equation (2.31). This region is called the excluded volume. The bigger the small particles are, the bigger the excluded volume surrounding the large particles. When the large particles get close to one another (such as the two large particles on the right in Figure 2.4), their excluded volume regions overlap. When excluded volume regions overlap, the total available volume for the smaller particles increases, which results in higher entropy for the system.

Because systems in equilibrium have maximum entropy, this causes the large particles to spontaneously move together. This is the depletion force present in all systems of particles of varying size (note that if the smaller particles were much, much smaller than the large particles, the excluded volume region would be very small and the depletion force would be very weak). [40, 41]. A similar effect has been seen for particles of the same size, so studying these types of systems is also important.

Depletion forces have effects on polymers in addition to systems of free-floating spheres, as many polymer models are simply hard-spheres connected together. This is true for systems of polymers in a solvent of crowding agents where the monomers and crowding agents have the same diameter. A reduction of average size of the polymer is observed in these systems[42]. When the crowding agents are smaller than the monomers, a full collapse of the polmyer is observed[29].

A study mentioned in the previous chapter[31] outlined an approximation for the effects of crowding agents on segregating polymers, suggesting that there are two effects of crowding agents that cancel each other out: (A) The depletion forces collapse the polymers and this compact form prevents each polymer from becoming entangled

with the other one, and (B) the osmotic forces from the crowding agents force the polymers to mix with one another[31]. The author thus argues that crowding agents should have no effect on polymer segregation. This is not what other studies have observed in practice[21], however, and is not what is observed in this study.

Chapter 3

Methods and Model

3.1 Methods

Computer simulations allow us to study intricate details of systems that may be difficult to study experimentally. Most often it is useful to use computer simulations when studying systems with a large number of particles, and this is relevant in polymer physics, where there may be very large numbers of monomers. With computer simulations, we are able to examine systems of very large polymers in reasonably short amounts of time.

The two most common methods of simulating the behaviour of polymers are molecular dynamics and Monte Carlo methods. The former is useful when studying time-dependent properties of a system, while the latter is useful in efficiently calculating static thermodynamic properties. In this chapter, we will discuss the particular methods used, and the model upon which we built our simulations.

3.1.1 Metropolis Monte Carlo

From classical statistical physics, the partition function for N particles can be written as

$$Q = c \int d\vec{p}^N d\vec{r}^N \exp[\beta H(\vec{p}^N, \vec{r}^N)] \tag{3.1}$$

where $H(\vec{p}^N, \vec{r}^N) \equiv H(\vec{p}_1, \vec{p}_2, ...\vec{p}_N, \vec{r}_1, \vec{r}_2, ...\vec{r}_N)$, and where c is a proportionality constant that depends on the details of a particular system[32]. The Hamiltonian, H is a sum of the potential and kinetic energy ($H = K + U$) Using the partition function, we can find the average value of an observable A.

$$\langle A \rangle = \frac{\int d\vec{p}^N d\vec{r}^N A(\vec{p}^N \vec{r}^N) \exp[-\beta H(\vec{p}^N, \vec{r}^N)]}{\int d\vec{p}^N d\vec{r}^N \exp[-\beta H(\vec{p}^N, \vec{r}^N)]} \tag{3.2}$$

Occasionally the partition function can be easily evaluated, but most of the time determining $\langle A \rangle$ analytically becomes impossible due to the complicated nature of equation (3.1). We are therefore left to solve equation (3.2) using other means. In particular, we can use Monte Carlo methods to do so.

We do not actually need the partition function to determine $\langle A \rangle$. Equation (3.2) illustrates that only a ratio of the two integrals is necessary. Metropolis et a. showed that it is possible to use Monte Carlo methods to find this ratio[32].

In this case it is only necessary to use the configurational part of the partition function (not dependent on momentum) where $A = A(\vec{r}^N)$. In the case where the quantity A depends only on position, $A = A(\vec{r}^N)$, the momenta can be integrated

$$\langle A \rangle = \frac{\int d\vec{r}^N A(\vec{r}^N) \exp[-\beta U(\vec{r}^N)]}{Z} \tag{3.3}$$

where

$$Z = \int d\vec{r}^N \exp[-\beta U(\vec{r}^N)], \tag{3.4}$$

and where Z is the configurational partition function and $U(\vec{r}^N)$ is the potential energy for a system in configuration $\vec{r}^N$.

The particle position probability density (also known as the Boltzmann distribution) is

$$P(\vec{r}^N) = \frac{\exp\left[-\beta U(\vec{r}^N)\right]}{Z}, \tag{3.5}$$

where $\beta = \frac{1}{k_B T}$. This equation tells us the probability that the system is in a particular state of position associated with the potential energy $U(\vec{r}^N)$[43].

If a sequence of states is generated such that the probability of visiting a state satisfies equation (3.5), then

$$\langle A \rangle \approx \frac{1}{L} \sum_{i=1}^{L} A(\vec{r}_i^N), \tag{3.6}$$

where L is the total number of generated points[32]. This equation becomes exact in the limit $L \to \infty$.

To do this, we start with a system (for example, an arrangement of particles) with a particular Boltzmann factor $\exp[-U_i(\vec{r}^N)]$. We then generate a new configuration for one or more of the particles by changing their position coordinates by a small amount. In this equation we must include all of the configurations of the system after each attempted move, even configurations that remain the same because a move was rejected. We decide whether to accept or reject this new configuration based on the Metropolis scheme described below.

When a system is in equilibrium, the probability that it is in a particular state must not change. This means that on average in a given series of state changes, the

number of transitions from state i to state j must equal the number of transitions from state j to state i. This condition is called "detailed balance"[32], and can be written

$$P_i g_{i\to j} p_{i\to j} = P_j g_{j\to i} p_{j\to i}. \tag{3.7}$$

This is the product of the probability that the system is in state i (P_i), the probability that a transition from state i to state j will be attempted ($g_{j\to i}$), and the probability that this movement will be accepted($p_{j\to i}$)[36]. Transitioning forwards and backwards between states must have equal probability.

The Metropolis algorithm is defined by the fact that the probability of attempting to transition from one state i to another state j is chosen to equal to the probability of attempting to transition from j to i. This means that $g_{i\to j} = g_{j\to i}$, and we can rewrite equation (3.7)

$$P_i p_{i\to j} = P_j p_{j\to i},$$

or

$$\frac{p_{i\to j}}{p_{j\to i}} = \frac{P_j}{P_i}.$$

Using equation 3.5, we get

$$\frac{p_{i\to j}}{p_{j\to i}} = \exp\Big[-\beta\Big(U_j(\vec{r}^N) - U_i(\vec{r}^N)\Big)\Big] \tag{3.8}$$

The Metropolis algorithm is also defined by the fact that if a transition is attempted to a state with a lower energy, it must always be accepted. If a transition is attempted from a lower energy state to a higher energy state, i.e. $U_j \leq U_i$, then the probability of it being accepted is determined by the above equation. This is

a particularly convenient choice that satisfies equation (3.8). The probability of a transition from one state to another can then be written

$$p_{i\to j} = \begin{cases} 1, & \text{if } U_j \leq U_i, \\ \exp\Big[-\beta\Big(U_j(\vec{r}^N) - U_i(\vec{r}^N)\Big)\Big], & U_j > U_i. \end{cases} \tag{3.9}$$

The particles in this project are the monomers of a polymer and the crowding agents. A trial move consists of an attempt to displace a monomer a small amount in the x, y, and z directions. This allows for movement of the polymer in space.

A special case of equation (3.9) arises due to the "hard" potentials (for example, 2.10):

$$p_{i\to j} = \begin{cases} 1, & \text{if no overlap}, \\ 0, & \text{if overlap} \end{cases} \tag{3.10}$$

because an overlap means that $\Delta U = \infty$.

3.1.2 Multiple Histogram Method

For our system, we want to know the free energy F as it changes with the distance between the centres of mass of the polymers , λ. This requires having a range of λ values from which we can calculate the free energy. We cannot find $F(\lambda)$ for all desired λ values in one simulation, as it is extremely improbable for the system to move to configurations at the top of the free energy barrier when this barrier is greater than a few k_BT. We would be left with many samples for certain λ values near the minimum, but very few (if any) for others, leading to very poor statistics. In order

to properly sample the range of λ values, we will use the self-consistent histogram method[32].

Rather than performing a simulation using the entire range of λ values, we can perform many smaller ones using smaller, equally-sized ranges where the free energy does not change significantly. We call these ranges 'windows', and by performing simulations in each one, we force the system to sample a wider range of configurations. We implement windows into the system using the following potential W_i:

$$W_i = \begin{cases} \infty, & \lambda < \lambda_i^{min} \\ 0, & \lambda_i^{min} < \lambda < \lambda_i^{max} \\ \infty, & \lambda > \lambda_i^{max}, \end{cases}$$

where λ_i^{min} and λ_i^{max} are the edges of the i^{th} window[32]. This means that the polymers must have a λ value inside the specified window. Any attempts to make a move that results in a λ that is too large or too small is rejected, as such a move would result in an infinite potential energy, which would be rejected based on equation (3.9). Each window is divided up into an equal number of bins, which are smaller ranges that are used to count how often λ is within a particular range. This allows us to discretize a continuous probability distribution into a probability histogram.

Each window overlaps with half of the window on the left, and half of the window on the right (except for the first and last window). This overlap is necessary for the algorithm[32], and the overlap width of $\frac{1}{2}$ was a choice for convenience. We can perform simulations for each window, obtaining a probability distribution for each one based on the counts in each bin. These probability distributions are then reconstructed into an overall probability distribution for the system using an algo-

rithm designed to minimize the accumulation of error[32]. From this, we are able to determine the free energy function

$$F(\lambda) = -k_B T \ln(P(\lambda)), \tag{3.11}$$

where $P(\lambda)$ is the overall probability distribution for a given λ.

3.2 Model

Modeling any physical system requires choices to be made regarding which details to include and which details to leave out, as it is necessary to strike a balance between realism and efficiency. In the case of a bacterial cell, there are many biological processes that cannot all be included in the model. This section will be an overview of the model and the details we have chosen to include.

3.3 Polymer Model

There are two polymers in this system, each consisting of N monomers bonded together in a ring. The polymers are made up of hard-sphere monomers, which means that the monomers cannot overlap with one another and are spherical in shape. For two monomers that are not bonded to each other, they are subject to the potential

$$U_{nb}(r) = \begin{cases} \infty, & r < \sigma \\ 0, & r \geq \sigma \end{cases} \tag{3.12}$$

where r is the distance between the centres of mass of two monomers, and σ is the diameter of each monomer. For monomers that are bonded to one another, they are

subject to a different potential

$$U_b(r) = \begin{cases} \infty, & r \leq 0.9\sigma \\ \infty, & r \geq 1.1\sigma \\ 0, & 0.9\sigma < r < 1.1\sigma. \end{cases} \tag{3.13}$$

Monomers that are bonded to one another have slightly fluctuating bond lengths, which was a convenient choice. Both of these potentials prevents monomers from overlapping with one another, and the second potential requires that the monomers stay bonded together in a polymer form.

This model does not include interactions at the atomic level, such as electrostatic interactions between monomers. While this level of detail would better reflect behaviour of real chromosomes, it is not necessary to include in a study of generic entropic effects.

Monomer movement is simulated using a Monte Carlo method described in the previous section. During the simulation, a random monomer is selected and attempted to move. There are three ways that monomers can be moved: translational moves, crankshaft moves, and global moves.

Translational Moves

If a translational move is attempted, a random distance up to 0.1σ is chosen in the $x, y,$ and z directions. The displacement along each axis is randomly chosen, so all three axes will have different displacements. We use a uniform distribution for $\Delta x, \Delta y$, and Δx centered at 0 (i.e. $\Delta x \in [-0.1\sigma, +0.1\sigma]$, $\Delta y \in [-0.1\sigma, +0.1\sigma]$, $\Delta z \in [-0.1\sigma, +0.1\sigma]$)

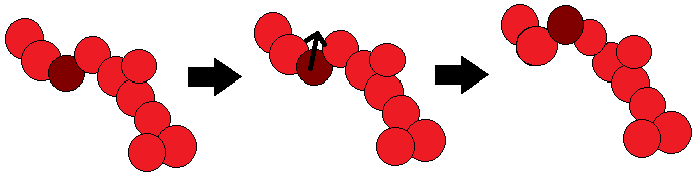

Figure 3.1: Translational move

Crankshaft Moves

For a crankshaft move, the two monomers adjacent to the selected monomer form an axis. The selected monomer is then rotated around this axis at a random angle between $-\pi$ and π radians with equal probability. No bond lengths are changed with this type of move.

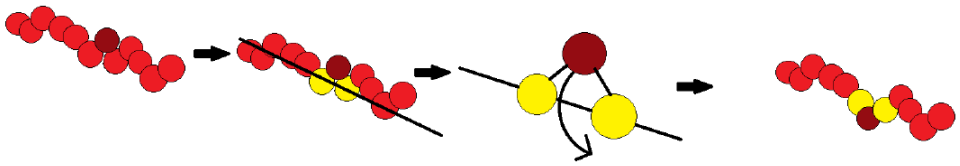

Figure 3.2: Crankshaft move

Global Moves

A global move is a translation of the entire polymer along the z axis (the axis parallel to the confinement). A distance up to 0.3σ in the positive or negative direction is selected and each monomer is displaced this amount along the z-axis. There is a uniform distribution for Δz centred at 0.

Finally, note that all three of these move types satisfy the requirement that $g_{i\to j} = g_{j\to i}$ mentioned previously.

3.4 Polymer Confinement

The polymers are confined in a cylindrical tube of radius R. The monomers are unable to overlap with this confinement. Because the monomers occupy volume and are not point particles, the centres of mass experience a smaller volume in which they can move around. The resulting radius becomes $R' = R - \frac{\sigma}{2}$. Figure 3.3 illustrates this effect.

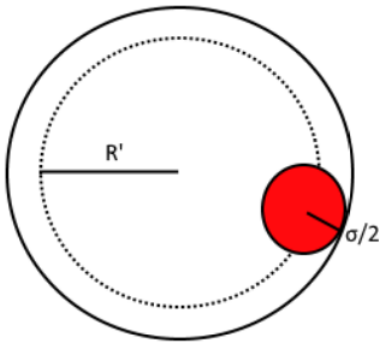

Figure 3.3: A cross-section of the tube, showing the effective radius (viewed from x–y plane).

For the first part of this study, the cylinder is infinitely long in the z direction. For the second part of this study, hemispherical caps are placed on either end of a cylinder of length L.

3.5 Crowding Agents

In Chapter 2 we discussed the purpose of including crowding agents into the model. In this study, the crowding agents and monomers have the same diameter (σ). These particles are hard spheres like the monomers, and are subject to the same potential of equation (3.12), where r is the distance between the centre of mass of a crowding agent and another crowding agent or monomer. The crowding agents cannot leave the confinement, just as monomers are unable to do so.

In order to keep the finite number of crowding agents at constant density inside an infinitely long cylinder, it was necessary to use periodic boundary conditions along the z axis in our system. This means that when a monomer or crowding agent crosses one of these boundaries, it appears on the other side. Figure 3.4 illustrates this with a system of two polymers and multiple crowding agents.

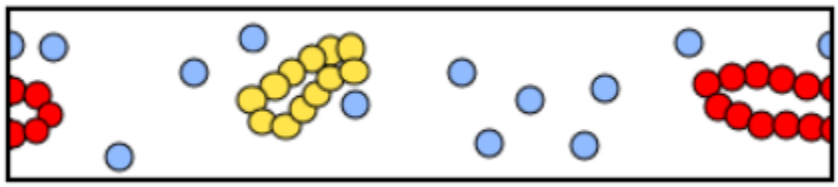

Figure 3.4: Periodic boundary conditions: when a particle moves past the boundary of one side, it reappears on the other side.

Using this method, the cylinder can still appear to be infinitely long (the objects within could travel forever along the z axis without stopping) with constant crowding agent density. This is achieved by creating images of the system on either side of the periodic boundary, which allows objects near one edge of the boundaries to be

checked for possible overlap with objects on the other side. These images are not 'real', as in this example there are still only two polymers in the system. The images are only used for move-checking purposes.

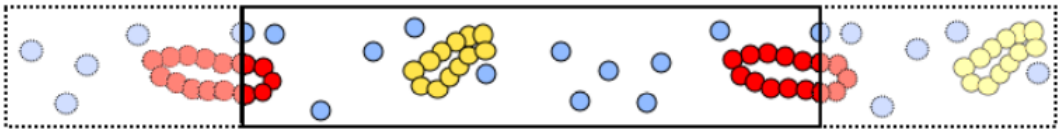

Figure 3.5: Periodic images: particles near the boundaries are checked for possible overlap using periodic images

The periodic boundary conditions were not used in the finite-length cylinder.

3.6 Simulation Details

We will now outline the process of the Monte Carlo simulation used in this study. In a previous section, we described the concept of windows. In this particular system, a window is chosen to be a specified range of allowed values for λ, the distance between the centres of mass of the two polymers. Many calculations are required, each for a given window.

The simulation progresses through cycles known as Monte Carlo cycles. One Monte Carlo cycle consists of N_p attempted moves, where N_p is the total number of particles in the system (monomers and crowding agents). At the beginning of each cycle, the type of particle chosen to move is selected. In our particular study, the probability a monomer will be chosen over a crowding agent is 0.7 (this choice was arbitrarily chosen). Once the type of particle is selected, a particular particle of that

type is randomly chosen to attempt a move. If the particle is a monomer, it may perform a translational, crankshaft, or global move. If the particle is a crowding agent, it may perform a translational move.

Once a move has been attempted, checks are made to see if the move is legal. The energy of a particle becomes infinite if any of the following conditions are true:

- a particle overlaps with another particle
- a particle attempts to leave the confinement (i.e. the attempted move places it past $R'-$see figure 3.3)
- the centre of mass of the two polymers has a value outside its acceptable window

Based on equation (3.9), a move that results in any of these conditions will be rejected (there is zero probability that such a move could occur). If none of these conditions are met, then the move results in a state with energy that is equal to the previous one. Based on equation (3.9), this move will be accepted.

In this study, there are N_{MC} Monte Carlo cycles performed during a simulation in a window. The first $0.1N_{MC}$ cycles are not used for calculations due the need of the system to equilibrate (reach equilibrium). This is because the polymer and crowding agents are initialized in an orderly arrangement that is very improbable. Because of this, the polymer and agents must go through many cycles before equilibrium is reached and the position of the particles are not influenced by their initial positions.

It is also not necessary to keep data from every Monte Carlo cycle, so to improve the speed of the calculations, only data from every 10 cycles is recorded.

3.6.1 Infinite Cylinder

For the infinitely long cylinder, there were typically 1.0×10^8 Monte Carlo cycles during a simulation for polymers of length $N = 80$ to 100. The first 1.0×10^7 cycles were considered to be equilibration cycles.

The maximum displacement of the monomers during translational moves was chosen to be 0.1σ, and the maximum displacement of the crowding agents was chosen to be 0.35σ. The maximum displacement for global moves varied depending on the particle density of the system, but was between 0.1σ and 0.3σ. These values were chosen in order to obtain acceptance ratios of approximately 0.5, which is the value for optimal efficiency in most systems[32].

The number of windows required depended on the number of monomers in the polymers, as longer polymers required λ to reach total segregation from one another. For polymers of $N = 60$, there were 20 windows. For polymers of $N = 100$, approximately 50 windows were required. Each window was 2.0σ wide.

3.6.2 Finite Cylinder

For the cylinder of finite length, there were typically 1.0×10^9 Monte Carlo cycles during a simulation for polymers of length $N = 80$ to 100. These simulations typically took longer than the cylinder of infinite length. The maximum displacement of the monomers during translational moves was chosen to be 0.1σ. Global moves were not performed during the simulations of the finite cylinder.

Chapter 4

Results and Discussion

In this chapter we will present and discuss the results of the Monte Carlo simulations of the systems of polymers in the infinitely long cylinder and cylinder of finite length. All distances are measured in units of σ and energy is measured in units of k_BT.

4.1 Cylinder of Infinite Length

Our first focus was to study a system of two polymers and multiple crowding agents confined to an infinitely long cylinder. We ran simulations for this type of system with varying polymer length, cylinder radius, and crowding agent density. Chain lengths from N= 50 – 100 were studied, with a focus on longer polymers (80 – 100 monomers). The cylinder radii studied were $R = 2, R = 2.5$, and $R = 3$. The crowding agent densities ranged from a density of $\rho_c = 0$ to approximately $\rho_c = 0.45$.

Figure 4.1 shows an example of a free energy calculation for a polymer of $N = 100$ and a crowding agent density of $\rho_c = 0.13$. The free energy decreases as the distance between the centres of mass increases. This trend was explained in detail in Chapter

2, and has been observed by others[10, 20, 34, 35]. The flat region at $\lambda = 0$ is the

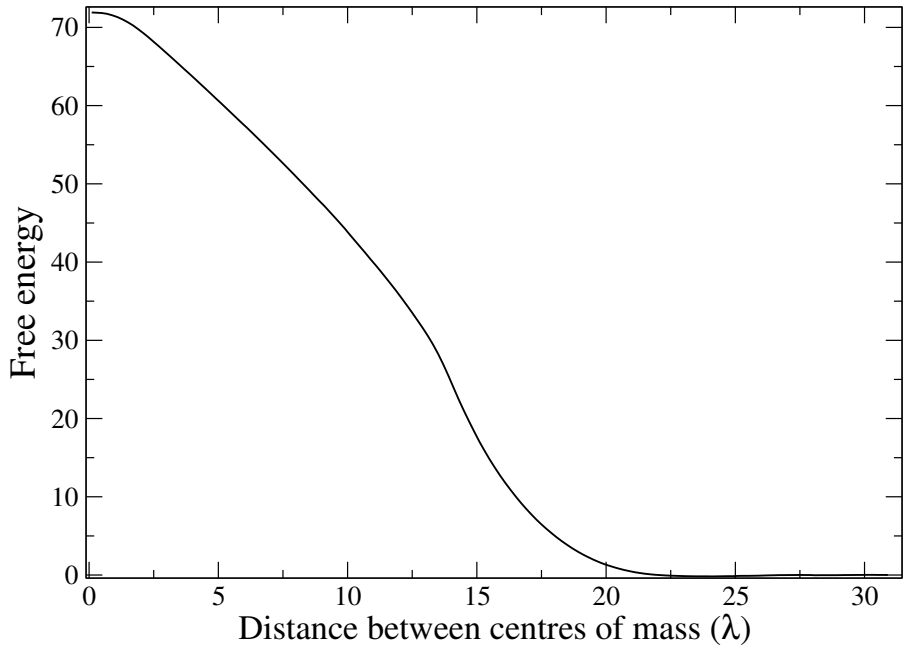

Figure 4.1: Free energy vs distance between centres of mass of polymers (λ) ($N = 80$, $R = 2.0$, $\rho_c = 0.2$

region of almost entire polymer overlap. This is where the polymers are most limited in possible configurations. In this region, one polymer tends to be more compacted than the other, with the longer polymer 'nesting' the other by extending past each end[10], as illustrated in Figure 4.2. The polymers tend to switch roles between the red and blue polymers shown in the figure. For small differences in λ, this nesting configuration does not change the degree of polymer overlap and so the free energy does not change.

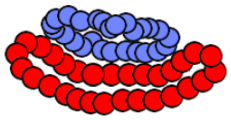

Figure 4.2: Illustration showing the red polymer nesting the blue polymer

As λ increases, F decreases due to the increased space for each polymer as they move away from one another. Between $\lambda = 2$ and $\lambda = 14$, this free energy decrease is roughly linear. At approximately $\lambda = 14$, the free energy decreases more rapidly. This change in the curve is due to the fact that the polymers have entered a regime in which they are in contact with one another but not overlapping, and they tend to be compressed along the direction of confinement. As the polymers continue to move apart, this compression decreases and the free energy decreases more quickly due to this increase of available space for the monomers. From $\lambda = 23$ onward, the polymers are completely segregated from one another and behave like two single confined polymers. Increasing λ has no effect on the free energy at this point.

The free energy trends remain the same with increasing crowding agent density. Figure 4.3 shows that the free energy barrier decreases as more crowding agents are added to the system. We can illustrate this behaviour in another fashion by plotting the free energy barrier height as a function of crowding agent density, as shown in Figures 4.4, 4.5, and 4.6. We define this height, ΔF, as $\Delta F = F(\lambda = 0) - F(\lambda = \infty)$. Note the behaviour of the $N = 100$ curve in Figure 4.5 between $\rho_c = 0.15$ and $\rho_c = 0.2$. Calculations were repeated at this point to determine if this behaviour could be repeated, and it was found each time. This bump does not make sense in the context of the other data, so further investigation will be necessary.

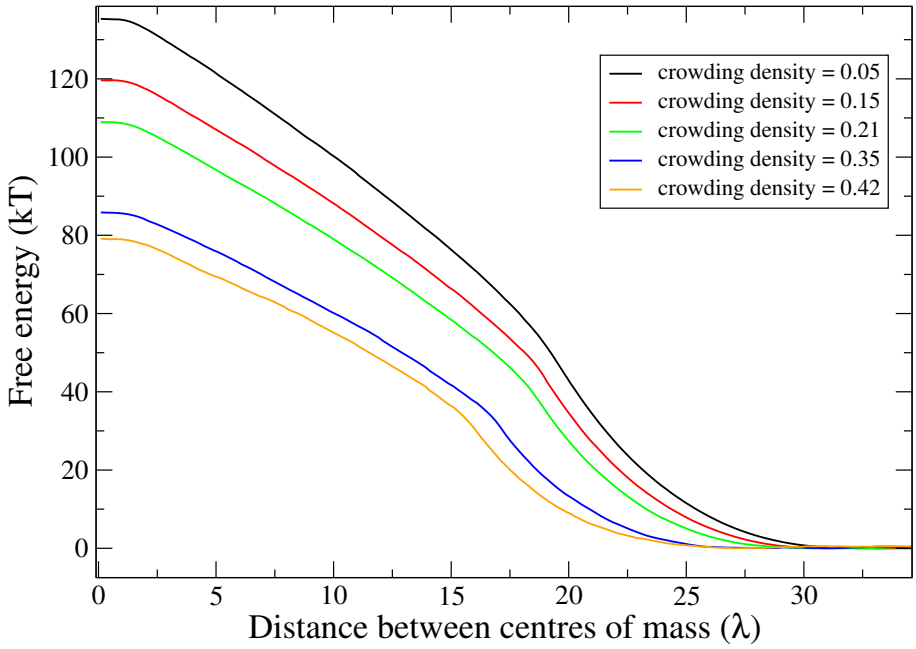

Figure 4.3: Free energy vs distance between centres of mass of polymers (λ) for polymers of $N = 100$ and a tube of radius $R = 2.0$, varying crowding agent density.

These results illustrate that the effect is present for varying cylinder diameter and crowding agent density. This effect was observed in a previous study that used finite-length cylinders [21], and we confirm these observations with our results using a wider range of parameters. These figures show that ΔF increases with N, and by comparing the graphs to one another, it is also apparent that ΔF decreases with D. This is qualitatively consistent with equation (2.26) from Chapter 2.

The reasons for this decrease in free energy with increasing crowding agent density is not completely clear. A possible contribution to this effect may be related to the

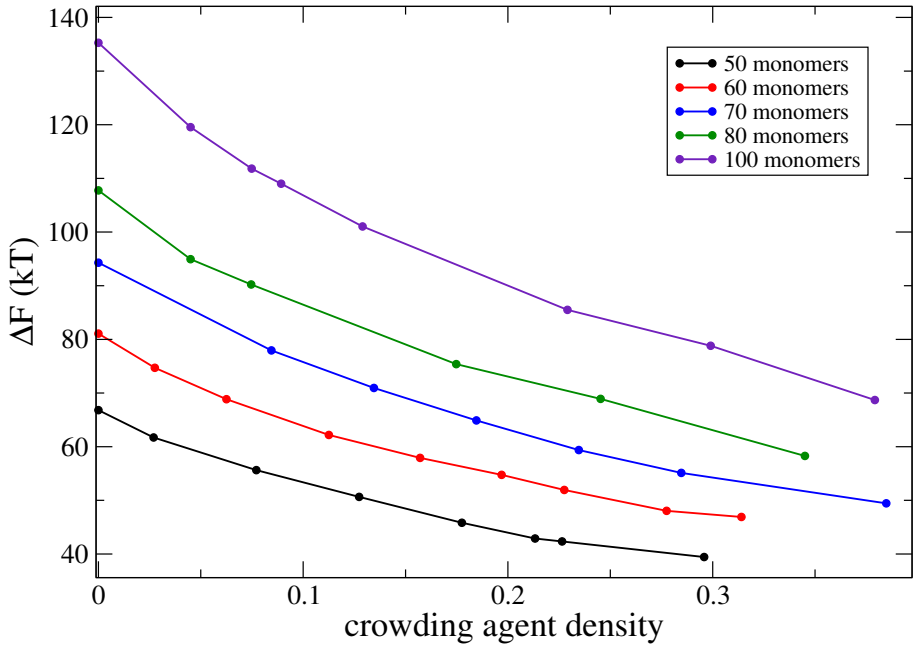

Figure 4.4: Free energy difference vs. crowding agent density for a cylinder of $R = 2.0$.

accessible volume of the crowding agents when the two polymers are overlapping compared to when they are segregated. When the polymers are overlapping with one another, the total length along the tube occupied by the polymer is less than the length along the tube they occupy when segregated. If crowding agents tend to be excluded from regions occupied by the polymers, then this means they have more volume to occupy when the polymers are overlapping. This would result in a decrease in free energy when the polymers are overlapping and an increase in free energy when they are segregated, because greater free volume means greater translational entropy for the crowding agents. This is the opposite trend to the free energy of the polymers,

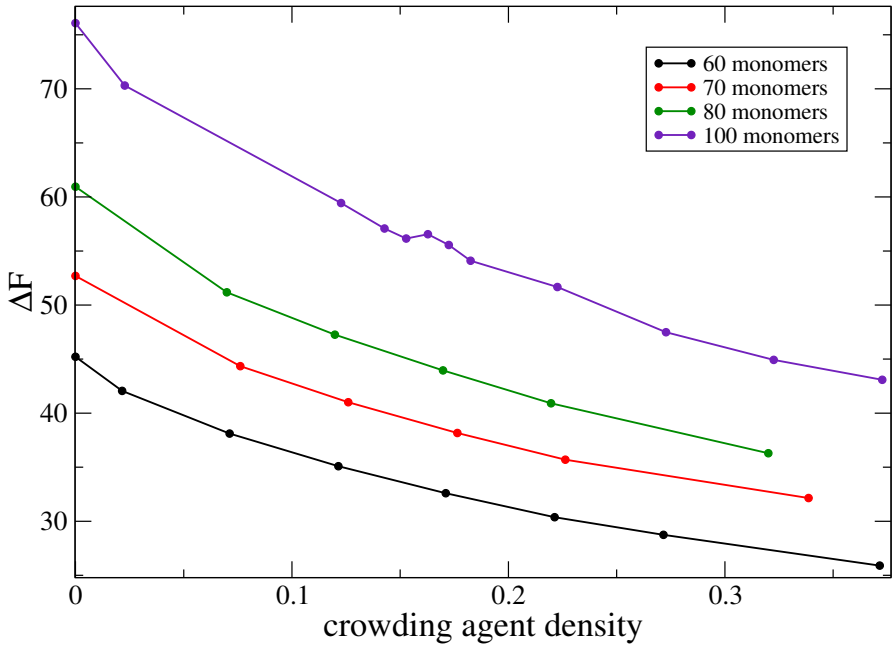

Figure 4.5: Free energy difference vs. crowding agent density for a cylinder of $R = 2.5$.

which we have shown have lower free energy when they are segregated. These two effects would then oppose each other and result in a lower free energy barrier at higher crowding agent density. Calculations must be performed to test that monomers are indeed excluded from the regions occupied by the polymers, however, and such calculations were not part of this project.

4.2 Cylinder of Finite Length

In addition to the cylinder of infinite length, we also examined a system of polymers confined to a cylinder of length L with hemispherical caps on either end. This was

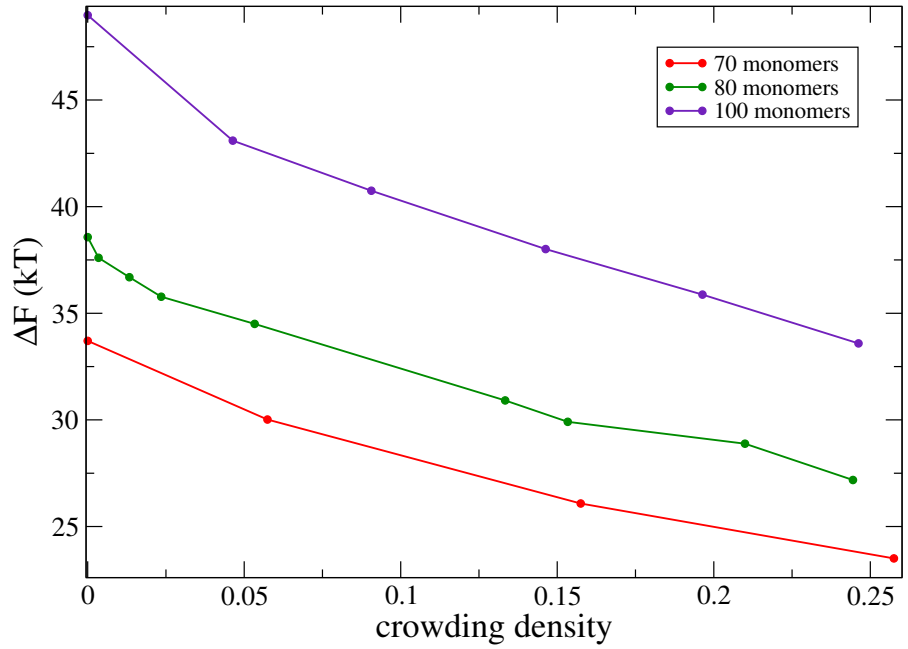

Figure 4.6: Free energy difference vs. crowding agent density for a cylinder of $R = 3.0$.

done to better model the environment of a bacterium, which obviously does not extend to infinity like the previous model. Studying tubes of infinite length and tubes of finite length allow us clearly identify all effects of confinement in the z direction. When the polymers segregate and move towards the ends of the cylinder, they are pushed against the ends and experience a large increase in free energy. This is reflected in Figure 4.7.

This trend was previously observed in systems that included crowding agents[21] and systems that did not[10]. This result illustrates that within a finite cylinder, the polymers do not attempt to get as far away from one another as possible. Rather,

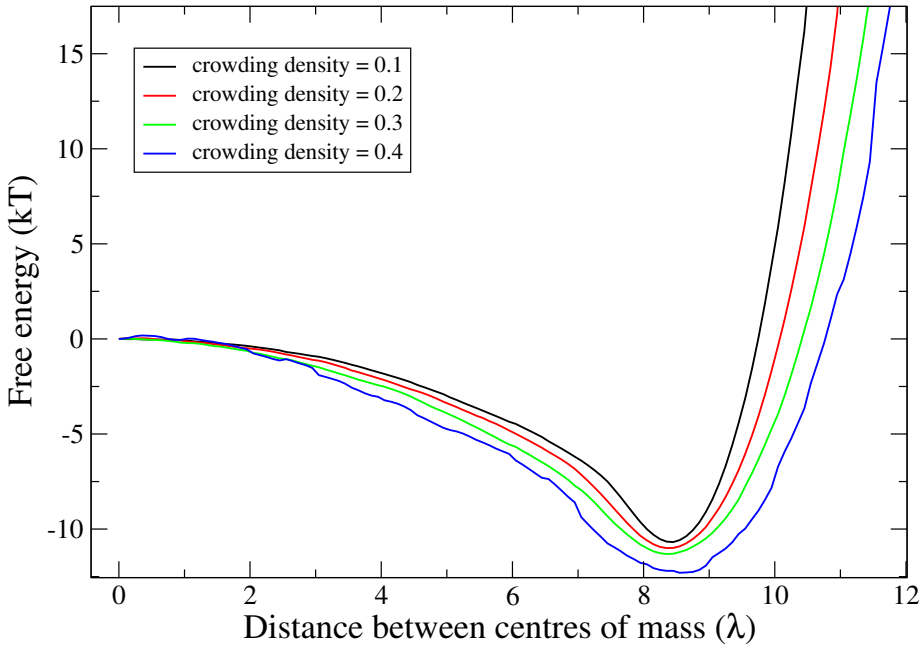

Figure 4.7: Free energy vs distance between centres of mass of polymers in a tube of finite length, $N = 100$, $R = 2.5$, $L = 14$.

there is a balance between polymer segregation and avoiding the hard caps at either end of the cylinder that results in polymer positions that minimize the free energy.

In Figure 4.7 we also see that the free energy difference increases with increasing crowding agent density, a trend that is opposite to what is seen when $L = \infty$ in the previous graphs (see the relevant curve in Figure 4.5 for the free energy trends for a system with the same number of monomers and tube diameter). This may be due to the very short length of the tube compared to the length of the confinement. The ρ_c curve has a noticeably lower quality than the other curves, and this is due to poorer statistics from the higher density. This high density requires shorter displacement

lengths in the Monte Carlo algorithm, which leads to more inefficient sampling. This can be remedied with much longer simulation runs at this density.

It has been found for systems where $N = 40$ that as L decreases, the effects of crowding become reduced[44]. It is possible that as L is further decreased and becomes very short with respect to N, the effects of crowding appear like they do in Figure 4.7. Calculations must be performed on systems with longer L to see if this trend continues, or if it reflects the trend with the infinitely long tube illustrated in previous graphs.

Chapter 5

Conclusion and Future Work

In this study, we calculated the free energy of a system of two polymers under confinement, examining both infinitely long and finite-length confining cylinders. This study was motivated by the lack of understanding of bacterial chromosome segregation, which is a seemingly simple phenomenon that may require an explanation based on physical mechanisms. Some suggest that spontaneous chromosome segregation occurs due to the entropy of chromosomes inside the bacterial cell, which is maximized when they are segregated from one another.

We modeled bacterial chromosomes using hard-sphered ring polymers inside cylinders of various diameter. We added crowding agents to our system, which were also hard spheres of the same size as the monomers. We found that in the infinitely long cylinder, the free energy barrier of the polymer system decreased as crowding agent density increased. In the finite cylinder, we found that the free energy rapidly increased as the polymers touched the caps on each side of the cylinder, which was expected. However, we also found that the free energy difference increased with in-

creasing crowding agent density, a result opposite to the trends found in systems of polymers in infinitely-long tubes. More calculations for the finite cylinder should take place for different lengths to determine the regime in which these unexpected results are found.

Other future work must include calculations to determine whether the free energy barrier decreases with increasing crowding agent density due to increased available volume for the crowding agents when the polymers are overlapping. Furthermore, similar free energy calculations should be made at larger cylinder diameter and longer cylinder length (for finite-length confinement) to determine how large the cylinder can be before the observed trends start to disappear.

It is also important to repeat these calculations using crowding agents that are smaller than the monomers, as this would provide insight into how depletion forces may play a role in segregation. Calculations with both infinitely long and finite-length cylinders should be performed with smaller crowding agents.

Finally, all of these calculations should be repeated for linear polymers, to understand how the ring topology affects the free energy of the polymer under various types of confinements.

This study was motivated by the issue of chromosome segregation in bacteria. Examining the free energy of segregating polymers, especially those in a confinement of finite-length, should be helpful in understanding chromosome segregation. In order for these calculations to be particularly meaningful, more calculations should be performed that more closely reflect the environment of a bacterial cell (particularly *E. coli*). For example, calculations for a cell with a realistic cell length/chromosome length ratio, realistic chromosome size/crowding agent size ratio, and realistic cell

crowding density could be especially useful for understanding the cell environment.

The results we have at present illustrate that even with highly crowded confinements, the polymers still have lower free energy when segregated from one another. This is promising because it still supports the original hypothesis that chromosome segregation in bacteria is largely due to a minimization of free energy.

Bibliography

[1] E. Robertis, F. Saez, and E. Derobertis, *Cell Biology* (Saunders, Philadelphia, PA, 1975).

[2] "From Prokaryotes to Eukaryotes", *Understanding Evolution* (University of California, Berkeley, CA, 2017).

[3] Image from the U.S. National Center for Biotechnology Information (Public domain in the United States).

[4] C. O'Connor, Nature Education **1**, 28 (2008).

[5] Yanagida, M. Philos Trans R Soc Lond B Biol Sci, **360**, 609-621 (2005).

[6] S. Jun and B. Mulder, Proc. Natl. Acad. Sci. USA **103**, 12388 (2006).

[7] S. Jun and A. Wright, Nat. Rev. Microbiol. **8**, 600 (2010).

[8] Y. Jung, J. Kim, S. Jun, and B.-Y. Ha, Macromolecules **45**, 3256 (2012).

[9] R. Reyes-Lamothe, E. Nicolas, and D. J. Sherratt, Annu. Rev. Genet. **46**, 121 (2012).

[10] J. M. Polson and L. G. Montgomery, J. Chem. Phys. **141**, 164902 (2014).

[11] G. Kaiser, "Electron Micrograph of a Bacterial Chromosome" *Doc Kaiser's Microbiology Website* (Community College of Baltimore County, MD, 1998).

[12] E. Minina and A. Arnold, Macromolecules **48**, 4998 (2015).

[13] R.M. Robertson, Single-Molecule Studies of DNA Dynamics and Intermolecular Forces, Ph.D. dissertation, University of California San Diego, 2007.

[14] P.J. Flory and W.R. Krigbaum, J. Chem. Phys. **18**, 1086 (1950).

[15] P.J. Flory, Principles of Polymer Chemistry (Cornell University Press, Ithaca, 1953).

[16] M. Daoud and P.D. Gennes, J. Phys. (Paris). **38**, 85 (1977).

[17] M. Muthukumar, Phys. Rev. Lett. **86**, 3188 (2001).

[18] A. Meller, L. Nivon, and D. Branton, Phys. Rev. Lett. **86**, 3435 (2001).

[19] W. Reisner, J.N. Pedersen, and R.H. Austin, Rep. Prog. Phys. **75**, 106601 (2012).

[20] Z. Benkov and P. Cifra, Biochm. Soc. Trans. Biochem. Soc. Trans. **41**, 625 (2013).

[21] J. Shin, A. G. Cherstvy, and R. Metzler, New J. Phys. **16**, 053047 (2014).

[22] Y. Jung and B.-Y. Ha, Phys. Rev. E **82**, 051926 (2010).

[23] P.A. Wiggins, K.C. Cheveralls, J.S. Martin, R. Lintner, and J. Kondev, Proc. Nat. Acad. Sci. USA. **107**, 4991 (2010).

[24] Y. Jung, C. Jeon, J. Kim, H. Jeong, S. Jun, and B.-Y. Ha, Soft Matter **8**, 2095 (2012).

[25] S.B. Zimmerman and L.D. Murphy, FEBS Lett. **390**, 245 (1996).

[26] J. Stavans and A. Oppenheim, Phys Biol. **3**, (2006).

[27] H.-X. Zhou, G. Rivas, and A.P. Minton, Annu. Rev. Biophys. **37**, 375 (2008).

[28] S.R. Mcguffee and A.H. Elcock, PLoS Comput Biol **6**, (2010).

[29] T.N. Shendruk, M. Bertrand, H.W. De Haan, J.L. Harden, and G.W. Slater, Biophys. J. **108**, 810 (2015).

[30] Y. Chen, W. Yu, J. Wang, and K. Luo, J. Chem. Phys. **143**, 134904 (2015).

[31] S. Jun, in *Bacterial Chromatin* (Springer Science+Business Media, Berlin, 2009), pp. 97113.

[32] D. Frenkel and B. Smit, Understanding Molecular Simulation: From Algorithms to Applications (Academic Press, San Diego, 2002), pp. 169-73.

[33] J.M. Polson, M.F. Hassanabad, and A. McCaffrey, J. Chem. Phys. **138**, 024906 (2013).

[34] J.M. Polson and A.C.M. McCaffrey, J. Chem. Phys. **138**, 174902 (2013).

[35] J.M. Polson and T.R. Dunn, J. Chem. Phys. **140**, 184904 (2014).

[36] M. Rubinstein and R.H. Colby, *Polymer Physics* (Oxford University Press, Oxford, 2003), pp. 49-54, 108.

[37] D. Schroeder, *Thermal Physics* (Addison Wesley Longman, Boston, 2001), pp. 74-75.

[38] T. Kawakatsu, *Statistical Physics of Polymers: An Introduction* (Springer, Berlin, 2011).

[39] Image by Aidan Tremblett, reproduced with permission.

[40] R. Ellis, Trends Biochem Sci **26**, 597 (2001).

[41] J.R.C. Maarel, Johan R. C. van der, *Introduction to Biopolymer Physics* (World Scientific, Singapore, 2008).

[42] F.A. Escobedo, Molecular Phys. 1996, **89**, 1733-54.

[43] R. Bowley and M. Sanchez, *Introductory Statistical Mechanics* (Clarendon Press, Oxford, 1999).

[44] J.M. Polson, (Private Communication)